ELSEVIER

Journal of Alloys and Compounds 220 (1995) 142–147

Journal of ALLOYS AND COMPOUNDS

Thermodynamics-based alloy design criteria for austenite stabilization and transformation toughening in the Fe–Ni–Co system

G.N. Haidemenopoulos [a], M. Grujicic [b], G.B. Olson [c], M. Cohen [d]

[a] *Department of Mechanical Engineering, University of Thessaly, Volos, Greece*

[b] *Department of Mechanical Engineering, Clemson University, Clemson, SC, USA*

[c] *Department of Materials Science and Engineering, Northwestern University, Evanston, IL, USA*

[d] *Department of Materials Science and Engineering, Massachusetts Institute of Technology, Cambridge, MA, USA*

Abstract

Transformation toughening has been widely applied in metastable austenitic steels. Recently this toughening mechanism has been extended to ultrahigh strength secondary-hardening martensitic steels, bearing suitable austenitic dispersions. The resulting dispersed-phase transformation toughening depends on the stability of the austenitic dispersions. The stability of dispersed austenite depends on various factors including the chemical composition and size of austenite particles, the stress state and the yield strength of the matrix. A single-parameter characterization of the stability of the austenitic dispersion is provided by the M_s^σ temperature and a functional form relating that temperature with the above-mentioned factors is developed. The microstructural requirements for dispersed-phase transformation toughening are then derived in terms of the austenite particle size and chemical enrichment in stabilizing solutes. Compositional effects on austenite stability have been studied by performing thermodynamic calculations using the Thermo-Calc software. The free-energy change $\Delta G^{ch} = G^{b.c.c.} - G^{f.c.c.}$ for martensitic transformation (a measure of austenite stability) has been evaluated as a function of composition in the ternary Fe–Ni–Co system. This information, when superimposed on isothermal sections at the tempering temperatures of interest, provides a way for selecting alloy compositions that maximize the thermodynamic stability of dispersed austenite.

Keywords: Alloy design; Transformation toughening; Dispersed austenite

1. Introduction

Transformation toughening is a toughening mechanism that has been successfully applied in metastable austenitic steels by Zackay and coworkers [1]. The mechanism of transformation toughening in these systems has been studied extensively by Leal [2]. Recently, this concept has been extended in ultrahigh strength martensitic steels, where transformation toughening is the consequence of the transformation of austenite dispersions [3]. Dispersed austenite can take two forms in steels. One form is the well-known "retained" austenite, which is the austenite that remains untransformed after the quench from the austenitizing temperature. Transformation plasticity and toughening effects associated with retained austenite have been studied recently [4,5]. The other form of dispersed austenite is the "precipitated" austenite which is the form of austenite that precipitates on high temperature tempering or intercritical annealing. The fundamental difference in the mode of formation of these two types of austenite makes the precipitated austenite attractive for the study of transformation toughening. Since it is formed through a precipitation reaction rather than being the leftover of a martensitic transformation, its amount and distribution can be controlled. Its size and composition can be varied through heat treatment and its stability can be tuned for transformation-toughening effects.

The most important parameter controlling the potential of dispersed austenite for transformation toughening effects is its thermodynamic stability. The stability depends on the following factors: (1) the chemical composition of the austenite particles (it affects the chemical driving force for the martensitic transformation); (2) the austenite particle size (it affects the

SSDI 0925-8388(94)06015-0

probability of finding nucleation sites in the particle); (3) the stress state (owing to the interaction of the transformational volume change with stress triaxiality); (4) the strength of the matrix (it affects the mechanical driving force contribution to the total driving force for the martensitic transformation).

In this work, the parameters which affect austenite stability are identified and a functional form relating austenite stability with these parameters is derived. For this purpose, a single-parameter characterization of austenite stability will be adopted and this is provided by the temperature M_s^σ defined below. Thermodynamic calculations employing the Thermo-Calc system [6] and using data from the work of Guillermet [7] for Fe–Ni–Co deal with the compositional effects on austenite stability. Alloy design criteria for transformation toughening are then presented based on thermodynamics.

2. Stability characterization

For the purpose of alloy design it is very important to develop a quantitative characterization of the stability of dispersed austenite. As the temperature M_s is used to characterize the stability of the austenite phase against martensitic transformation on cooling, another parameter, the temperature M_s^σ, can be used to characterize the stability of dispersed austenite against martensitic transformation under the action of applied stress. M_s^σ is defined as the temperature at which the stress required for stress-assisted martensitic transformation equals the yield strength of the parent austenite phase [8].

M_s^σ depends on the size and composition of the austenite particles, the yield strength of the matrix and the stress state:

$$M_s^\sigma = M_s^\sigma\left(\sigma_y, \frac{\sigma_h}{\bar{\sigma}}, V_p, \text{wt.\% Ni}\right) \tag{1}$$

where σ_y is the yield strength, σ_h is the hydrostatic stress, $\bar{\sigma}$ is the effective stress and V_p is the average austenite particle size.

Experiments in homogeneous metastable austenitic steels [2] have shown that maximum toughening occurs when M_s^σ for the crack tip stress state is just below room temperature. The required microstructure can then be prescribed by model predictions of M_s^σ for the Fe–Co–Ni system of interest to this work. A functional form will be developed for M_s^σ in Eq. (1) that will enable the prediction of required particle size and Ni enrichment to set $M_s^\sigma = 300$ K.

For the case of stress-assisted nucleation, the applied elastic stress assists the transformation kinetics by modifying the effective potency distribution of the pre-existing nucleation sites. Based on a dislocation dissociation model of classical heterogeneous martensitic nucleation via elastic interactions with internal stress concentrations [9], the potency of a nucleation site can be expressed in terms of the thickness n (in numbers of crystal planes) of the nucleus that can be derived from the defect by barrierless dissociation. The critical n for nucleation at a given thermodynamic driving force per unit volume ΔG^{ch} is

$$n = -\frac{2\gamma_s/\rho}{\Delta G^{ch} + E^{str} + W_f} \tag{2}$$

where γ_s is the nucleus specific interfacial energy, ρ is the density of atoms in a closed-packed plane, E^{str} is the elastic strain energy per unit volume associated with distortions in the nucleus interface plane and W_f is the frictional work of interfacial motion. Based on this model, Cohen and Olson [10] derived the cumulative structural defect-potency distribution $N_v(n)$, from the Cech and Turnbull [11] small-particle experiments in Fe–30 wt.% Ni:

$$N_v = N_v^0 \exp(-\alpha n) \tag{3}$$

where N_v^0 is the total number of nucleation sites of all potencies and α is a constant.

The effect of the applied stress on the potency distribution can be found by adding a mechanical driving force term ΔG^σ to the chemical driving-force term ΔG^{ch} in Eq. (2), to obtain the total driving force

$$\Delta G = \Delta G^{ch} + \Delta G^\sigma \tag{4}$$

The mechanical driving force is related to the applied stress through the expression

$$\Delta G^\sigma = \sigma \frac{\partial(\Delta G)}{\partial \sigma} \tag{5}$$

According to the assumption by Patel and Cohen [12] that the operative nucleation sites are of the optimum orientation for maximum interaction with the applied stress, then $\Delta G^\sigma = \Delta G_{max}{}^\sigma$ for all sites.

The stress-assisted transformation of a well-spaced dispersion of metastable particles in a stable matrix is controlled by the pre-existing nucleation sites for which the potency distribution under an applied elastic stress σ is given by Eq. (3). For an average particle volume V_p, the fraction of particles to transform via sites of a potency with a cumulative number density N_v is equal to the probability of finding at least one nucleation site in the particle, assuming that a single nucleation event transforms the particle to martensite. This probability is

$$f = 1 - \exp(-N_v V_p) \tag{6}$$

The transformation stress σ_t can then be found by combining Eqs. (2)–(6):

$$\sigma_t = \frac{1}{\partial(\Delta G)/\partial\bar{\sigma}} \times \left(\frac{2\alpha\gamma_s/\rho}{\ln[-[\ln(1-f)]/N_v^0 V_p]} - \Delta G^{ch} - W_f - E^{str} \right) \quad (7)$$

The chemical driving force can be expressed as a function of temperature and weight percentage of Ni using the Thermo-Calc database. For the Fe–14wt.%Co system a linear expression was obtained as follows:

$$\Delta G^{ch} = -8885.82 + 200.48(\text{wt.\% Ni}) + 5.91T \quad (8)$$

The frictional work W_f of interfacial motion was calculated as a function of Ni content from the composition dependence of the critical driving force ΔG_{crit} at M_s for Fe–Ni alloys [13]:

$$W_f = 2.93(\text{wt.\% Ni})^{2/3} \quad (9)$$

The parameter $\partial(\Delta G)/\partial\sigma$ is given as a function of stress state by Olson and Cohen [14] as follows: for compression -0.58 J mol^{-1} MPa^{-1}, for tension -0.86 J mol^{-1} MPa^{-1} and for the crack tip -1.42 J mol^{-1} MPa^{-1}. If the stress state is represented by the parameter $\sigma_h/\bar{\sigma}$, then a straight-line fit of the data gives

$$\frac{\partial(\Delta G)}{\partial\bar{\sigma}} = -0.715 - 0.3206\frac{\sigma_h}{\bar{\sigma}} \quad (10)$$

At M_s^σ, the transformation stress equals the yield stress. Setting $\sigma_t = \sigma_y$ and substituting Eqs. (8)–(10) into Eq. (7), M_s^σ can be obtained as follows:

$$M_s^\sigma = \sigma_y\left(0.121 + 0.0542\frac{\sigma_h}{\bar{\sigma}}\right) + \frac{1465.3}{-4.6 - \ln(N_v^0 V_p)} + [1418.92 - 33.92(\text{wt.\% Ni}) - 0.5(\text{wt.\% Ni})^{2/3}] \quad (11)$$

This equation shows the effects of yield strength, stress state, austenite particle size and Ni enrichment on the stability of the dispersed austenite as expressed by M_s^σ. It indicates that in order to obtain a very high stability of the dispersed austenite, so that M_s^σ for the crack tip stress state can be as low as room temperature, the austenite has to be very fine (small V_p) and enriched in Ni. The relationship between particle size and compositional enrichment can now be explored with the aid of Eq. (11).

If we take as a model system the AF1410 steel with composition Fe–14wt.%Co–10wt.%Ni–2wt.%Cr–1wt.%Mo–0.16wt.%C and yield strength 1400 MPa, set $M_s^\sigma = 300$ K for the crack tip stress state, and take $\sigma_y = 1400$ MPa, the resulting relationship is indicated in Fig. 1 which shows the Ni content of the austenite particles vs. their size. The size here is represented by a scaled radius $(N_v^0 V_p)^{1/3}$. The figure indicates that the destabilizing effect of increasing the austenite particle

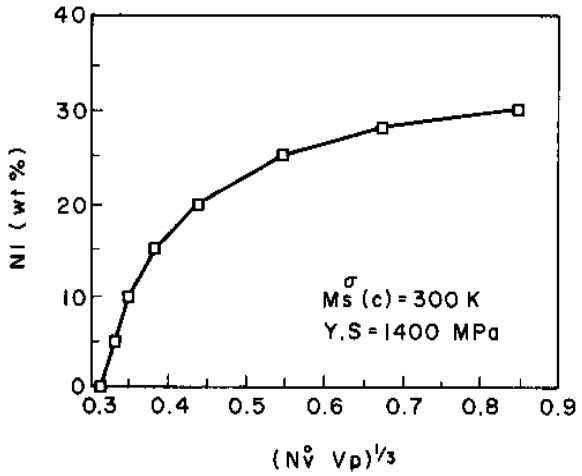

Fig. 1. Normalized austenite particle volume vs. Ni content in the Fe–14wt.%Co–10wt.%Ni system, for a yield strength of 1400 MPa and a crack tip M_s^σ of 300 K.

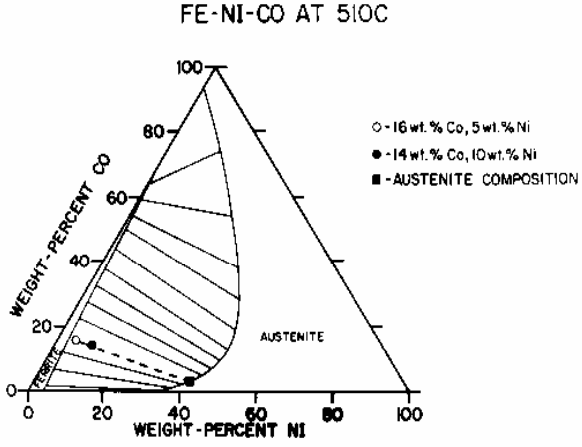

Fig. 2. Ternary section of the Fe–Ni–Co system at 510 °C computed with the Thermo-Calc software. ●, 14wt.%Co–10wt.%Ni alloy composition; ■, the austenite composition.

size should be compensated by a corresponding increase in Ni enrichment to keep the degree of stability constant. The parameter N_v^0 represents the total number of nucleation sites of all potencies. Its magnitude is not known for dispersed systems; however, the value 2×10^{17} m^{-3} has been obtained for Fe–Ni polycrystals [15]. Experimental results on the size and composition of austenite particles can be used to estimate the value of N_v^0 for the dispersed austenite.

3. Thermodynamic calculations

This section presents thermodynamic calculations regarding the compositional effects on austenite stability. The calculations were performed with the Thermo-Calc system. Figs. 2 and 3 show two isothermal sections of the ternary Fe–Ni–Co system at 510 °C and 600 °C respectively. The $(a+\gamma)$–γ phase boundary shifts to

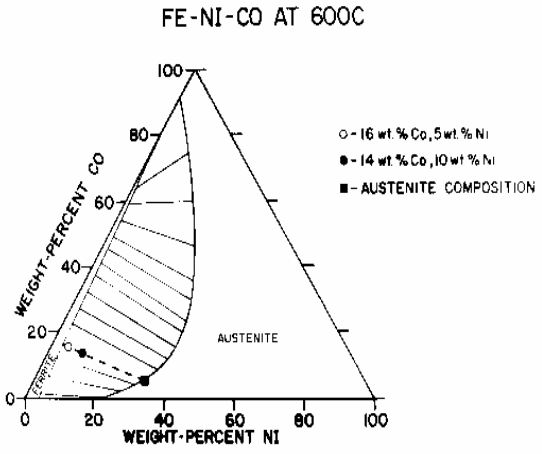

Fig. 3. Ternary section of the Fe–Ni–Co system at 600 °C computed with the Thermo-Calc software: ●, 14wt.%Co–10wt.%Ni alloy composition; ■, the austenite composition.

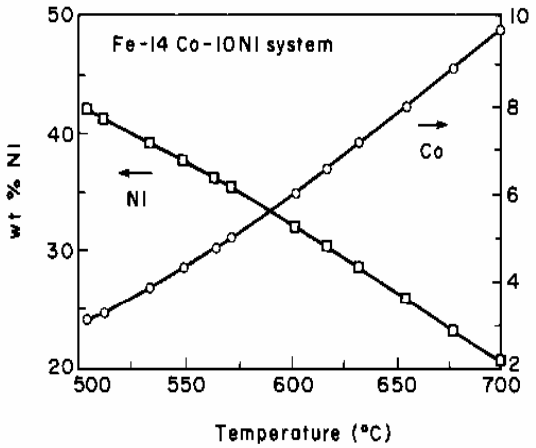

Fig. 4. Composition of the austenite as indicated by the weight percentages of Ni and Co in equilibrium with ferrite as a function of tempering temperature in the Fe–14wt.%Co–10wt.%Ni system. The calculations were performed using the Thermo-Calc software.

the left as the temperature is raised from 510 to 600 °C. This causes the Ni content of the austenite in equilibrium with ferrite to decrease. Therefore the austenite has a lower stability at higher temperatures.

The intersections of the tie-lines with the $(a+\gamma)$–γ two-phase boundary in Fig. 3 define the austenite compositions in equilibrium with ferrite at a given temperature. The locus of these intersection points as a function of temperature for the Fe–14wt.%Co–10wt.%Ni system is shown in Fig. 4. As the tempering temperature decreases, the austenite is enriched in Ni and depleted in Co. Fig. 5 shows the amount of austenite (mole fraction) as a function of tempering temperature, indicating that at the tempering temperatures of interest (500–600 °C), about 20% austenite can form at equilibrium.

Specific calculations were performed for the six-component AF1410 steel. Table 1 gives the calculated compositions and volume fractions of the equilibrium

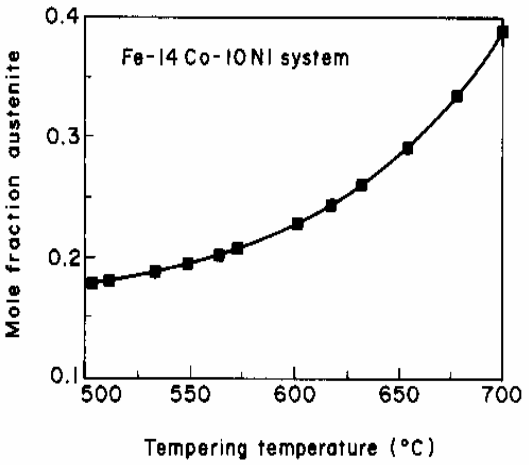

Fig. 5. Mole fraction of austenite as a function of tempering temperature in the Fe–14wt.%Co–10wt.%Ni system. The austenite is in equilibrium with ferrite. The calculations were performed using the Thermo-Calc software.

Table 1
Composition and volume fraction of equilibrium austenite in AF1410 steel at 510 and 600 °C

	510 °C	600 °C
Ni (wt.%)	38.50	27.60
Co (wt.%)	4.10	6.79
C (wt.%)	5.4×10^{-4}	8.5×10^{-3}
Cr (wt.%)	0.98	1.33
Mo (wt.%)	0.23	0.27
Fe (wt.%)	Balance	Balance
Volume fraction	0.167	0.240

austenite at 510 and 600 °C, while Table 2 gives the calculated compositions and volume fractions of the other phases in equilibrium with austenite at the same temperatures. The austenite is more enriched in Ni at 510 °C than at 600 °C but has a lower volume fraction at 510 °C.

Since the material is designed for transformation toughening at room temperature, a quantitative characterization of austenite stability that can also be used for alloy design can be provided by the free-energy change for martensitic transformation evaluated at room temperature. This quantity $\Delta G^{ch}(RT)$ was calculated for the Fe–Ni–Co system. The martensitic phase was represented by the b.c.c. phase with the same composition as the f.c.c. phase since the transformation is diffusionless. Fig. 6 shows the contours of the free energies of f.c.c. and b.c.c. phases as a function of composition, evaluated at 300 K. The difference between these free energies is the free-energy change for the martensitic transformation: $\Delta G^{ch} = G^{b.c.c} - G^{f.c.c.}$. The more positive this quantity, the more stable is the austenite. Fig. 7 shows contours of ΔG^{ch} as a function of composition for the ternary Fe–Ni–Co system. Superimposed on the same plot is the isothermal section

Table 2
Compositions and volume fractions of phases in equilibrium with austenite at 510 and 600 °C in AF1410 steel (the numbers in parentheses are for 600 °C)

	B.c.c.	$M_{23}C_6$	M_2C	M_6C
Ni (wt.%)	4.45 (4.61)			
Co (wt.%)	16.58 (16.92)			
Cr (wt.%)	0.51 (0.70)	52.20 (42.62)	19.71 (26.71)	5.26 (7.36)
Mo (wt.%)	0.14 (0.19)	20.21 (19.89)	73.37 (65.87)	68.51 (64.46)
C (wt.%)	8×10^{-5} (1.23×10^{-3})	5.06 (5.03)	6.87 (7.22)	2.48 (2.54)
Volume fraction	0.803 (0.703)	0.025 (0.024)	0.0042 (0.0046)	2.1×10^{-4}

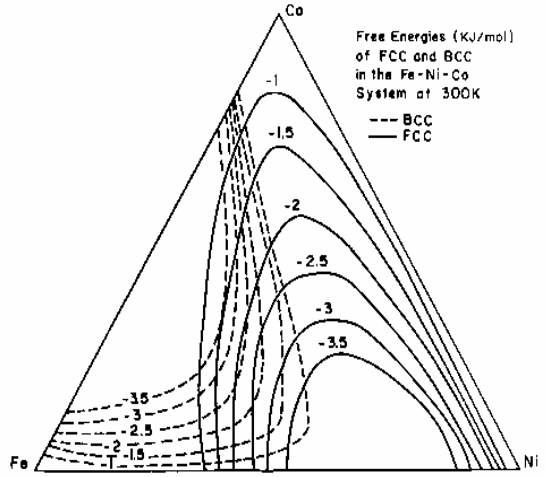

Fig. 6. Free-energy contours (in kilojoules per mole) of the f.c.c. and b.c.c. phases in the Fe–Ni–Co system at 300 K.

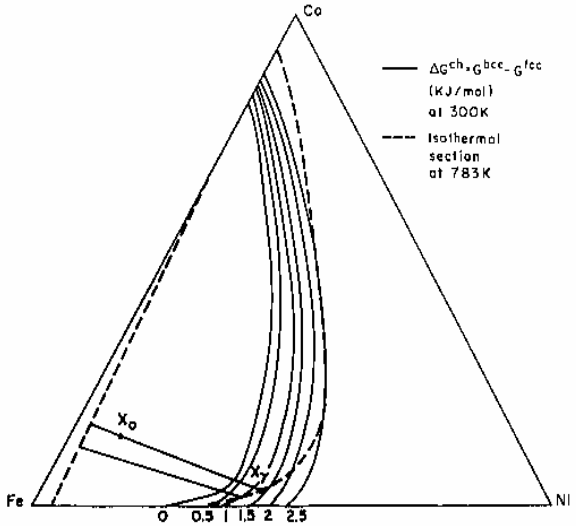

Fig. 7. Contours of the free energy change (in kilojoules per mole) for the martensitic transformation at 300 K (—) and superimposed isothermal section (– – –) at 783 K (510 °C) of the Fe–Ni–Co system. X_0 represents the alloy composition while X_γ represents the composition of austenite that forms at 510 °C.

of Fe–Ni–Co at 510 °C (broken curves) with two tie-lines shown. This combined plot allows one to select alloy compositions for austenite stabilization. Starting with an alloy composition X_0, the corresponding tie-line defines the composition X_γ of the austenite that precipitates at 510 °C. That composition then defines, from the ΔG^{ch} contour plot, the chemical driving force at room temperature. Table 3 lists alloy compositions with the corresponding values of ΔG^{ch}(RT) and volume fraction of austenite that precipitates at 510 °C. These results indicate that, for constant Co content, increasing the Ni content (e.g. from 10 to 15 wt.%), the austenite stability as well as its volume fraction increased. Increasing the Co content (e.g. from 14 to 18 wt.%) causes a further increase in the austenite stability but a corresponding decrease in austenite volume fraction. If the alloy design criterion is maximum austenite stability, then from Table 3 a Fe–18Co–15Ni matrix composition would be selected for transformation toughening.

Table 3
Alloy compositions, corresponding stabilities ΔG^{ch}(RT) and volume fractions of equilibrium austenite at 510 °C

Alloy composition (wt.%)	ΔG^{ch}(RT) (kJ mol^{-1})	Volume fraction of austenite
Fe–14Co–10Ni	1.1	0.177
Fe–14Co–15Ni	1.2	0.300
Fe–18Co–10Ni	1.4	0.172
Fe–18Co–15Ni	1.6	0.291

4. Conclusions

The stability of dispersed austenite is characterized by M_s^σ which depends on the austenite particle size and composition, the stress state and the yield strength. From the analysis presented in this work it is concluded that, in order to achieve very high stability of dispersed austenite for crack tip interactions, the austenite particles must be very fine and enriched in Ni. The tempering temperature at which the austenite precipitates is an important factor. At higher tempering temperatures the volume fraction of precipitated austenite increases but the austenite is less stable. Finally increasing the Ni content in the alloy causes an increase in both the

volume fraction and the stability of precipitated austenite while a corresponding increase in the Co content causes a further increase in austenite stability but a decrease in volume fraction. The analysis presented in this work provides a way for selecting alloy compositions for maximizing dispersed austenite stability and hence transformation toughening.

References

[1] W.W. Gerberich, P.L. Hemmings and V.F. Zackay, *Metall. Trans., 2* (1971) 2242.

[2] R.H. Leal, Transformation toughening of metastable austenitic steels, *Doctoral Thesis,* Massachusetts Institute of Technology, Cambridge, MA, 1984.

[3] G.N. Haidemenopoulos, G.B. Olson and M. Cohen, Dispersed-phase transformation toughening in ultrahigh-strength steels, in G.B. Olson, M. Azrin and E.S. Wright (eds.), *Proc. 34th Sagamore Army Materials Conf. on Innovations in Ultrahigh-Strength Steel Technology, Lake George, NY, 1990,* 1990, p. 549.

[4] G.N. Haidemenopoulos, M. Grujicic, G.B. Olson and M. Cohen, Transformation microyielding of retained austenite, *Acta Metall., 37* (6) (1989) 1677.

[5] G.N. Haidemenopoulos, G.B. Olson, M. Cohen and K. Tsuzaki, Transformation plasticity of retained austenite in stage-1 tempered martensitic steels, *Scr. Metall., 23* (1989) 297.

[6] B. Sundman, B. Jansson and J.O. Anderson, *Calphad, 9* (1985) 153.

[7] A.F. Guillermet, *Calphad, 13* (1989) 1.

[8] G.B. Olson, Mechanically-induced phase transformations in alloys, in M.B. Bever (ed.), *Encyclopedia of Materials Science and Engineering,* Pergamon, Oxford, 1986, pp. 2929–2932.

[9] G.B. Olson and M. Cohen, *Metall. Trans. A, 7* (1976) 1897.

[10] M. Cohen and G.B. Olson, Martensitic nucleation and the role of the nucleating defect, *New Aspects of Martensitic Transformations, First Japan Institute of Metals Int. Symp. Kobe, 1976,* in *Trans. Jpn. Inst. Met., Suppl., 17* (1976) 93.

[11] R.E. Cech and D. Turnbull, *Trans. AIME, 206* (1956) 124.

[12] J.R. Patel and M. Cohen, *Acta Metall., 1* (1953) 531.

[13] B.V. Narasimha Rao and G. Thomas, *Proc. Int. Conf. on Martensitic Tansformations, Cambridge, MA, 1979,* MIT Press, Cambridge, MA, 1979.

[14] G.B. Olson and M. Cohen, *Metall. Trans. A, 13* (1982) 1907.

[15] L. Kaufmann and M. Cohen, *J. Met.,* (1956) 1393.